A Geomorphology-Based Distributed Hydrologic Model and Its Application to Chao Phraya River Basin

D. Yang, S. Herath, K. Musiake
Institute of Industrial Sciences, University of Tokyo, Tokyo, Japan

Abstract

Differing from the discrete grid system, an alternative hillslope discretization scheme is adapt in the distributed hydrological model. This discretization scheme is based on the catchment area function and width function. The catchment is divided into a number of flow intervals along the flow distance. A flow interval is simply represented as a series of symmetric hillslope elements, the number of hillslope elements is determined by the number of river segments with the same flow interval (given by width function). The river network is lumped and the main channel is used as the equivalent river for routing the river flow. The catchment spatial variations, such as topography, land use and rainfall, are represented by one-dimensional distribution functions similar to area function. The hydrologic processes that occur in the hillslope elements are described by the physically-based governing equations. The runoff generated from the hillslope element is the lateral inflow of the river. The kinematic wave method is adapted to solve the river routing. The comparison of grid-based and geomorphology-based hydrologic models are discussed. Application to a large tropic river basin, Chao Phraya River in Thailand, is presented in the paper.

1. Introduction

Owing to the highly nonlinear nature of hydrologic processes and their mutual interactions, the hydrologic phenomena show a high degree of variability over a very wide range of space and time scales. So, the physically based descriptions of hydrologic processes are necessary to be incorporated in hydrologic modeling, and an appropriate approach is needed for representation of spatial heterogeneity.

Due to recent advance in GIS, remote sensing, hydrologic data base as well as computer hardware technology, the physically-based distributed hydrologic models becomes popular. A distributed physically-based model does not consider the water flows in a catchment to take place between a few storage units. Instead, the flows of water and energy are directly calculated from the governing continuum equations, such as the Saint Venant equations for overland and channel flow, Richards' equation for unsaturated zone flow and Boussinesq's equation for groundwater flow. Distributed physically-based models give a detailed and potentially more correct description of the hydrologic processes in the catchment than do the other model types. Moreover, they are able to use as much as possible of the information and knowledge that is available concerning the catchment that is being modeled. The geographic information system (GIS) and remote sensing are two major techniques to support this modeling approach. Today, several general purpose catchment model codes of this type exist such as MIKE SHE (Refsgaard, 1995), IHDM (Beven, 1987) and TOPMODEL (Beven, 1989).

The most common distributed hydrologic models employ a regular discrete square grid system to represent the spatial heterogeneity. The grid is the fundamental unit in hydrologic model. A typical representative of this type of distributed hydrologic model is MIKE SHE which developed by Danish Hydraulic Institute. The catchment geomorphologic area function and width function show the aggregating pattern of the catchment. They provide a possibility to quantitatively describe the catchment heterogeneity (Yang et al., 1997a). Naden (1992) described the rainfall and soil spatial distributions using weighted width functions in a hydrologic model. Yang et al. (1997b) used area function to describe the rainfall distribution for modeling flood by coupling with the tank model. In these treatments, spatial variables were represented by one dimension distribution functions with respect to the flow distance from the outlet. This description is simpler than discrete grid system (regular square grids), but it grasps the catchment geomorphologic characteristics.

The basic considerations of development of the hydrologic model in the study include: (1) distributed representation of spatial variations; (2) physical descriptions of hydrologic processes; (3) applicability to very large catchments (Yang, et al., 1998a). The hydrologic model is based on the one dimensional representations of catchment spatial variations by incorporating the catchment geomorphologic area function which is extracted from DEMs. The lateral dimension of the catchment is reduced from two to one dimension and the river network is lumped as a single equivalent channel. The computational unit is hillslope element instead of the grid in grid-based distributed model. This is an alternative type of distributed hydrologic model.

2. Grid Based Model

MIKE SHE is a comprehensive deterministic, grid-based distributed modeling system for the simulation of the land based part of the hydrologic cycle. It is applicable to a wide range of water resources and environmental problems. Water Movement (WM) is the basic module of the entire MIKE SHE system. It simulates the variations in hydraulic heads, flows and water storage in the entire land phase of the hydrologic cycle, viz. on the ground surface, in rivers and in the unsaturated and saturated subsurface zones. The catchment characteristics and input data are represented in a network of grid squares as shown in Figure 1. MIKE SHE uses a simple degree-day model for snowmelt, kinematic wave model for surface flow and river flow which is solved by implicit finite difference method, 1-dimensional Richards equation for describing unsaturated water flow that is solved by implicit scheme, and 3-dimensional groundwater flow.

In order to describe the topographical characteristics of the catchment accurately, the grid size should be defined appropriately and limited within an acceptable range. And this results a large computation demand of this type of distributed hydrologic models, which is a deterrent to apply to large scale.

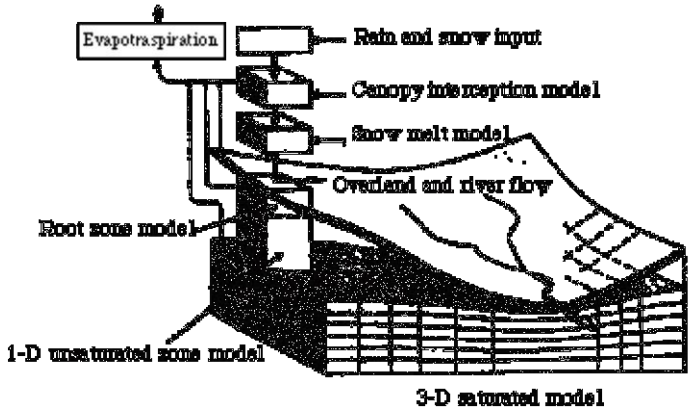

Fig. 1 Model Structure of MIKE SHE

3. Description Geomorphology-Based Hydrologic Model

3.1 Discretization of Catchment

When the river network is generated using flow accumulation method from grid-based DEM, the flow direction in each grid is determined according to the steepest descent direction. Following the flow direction, the flow distance of each grid from the outlet can be calculated. Then, the area function can be uniquely derived according to the flow distance. Figure 2(a) shows the flow distance contour map and area function of an example catchment.

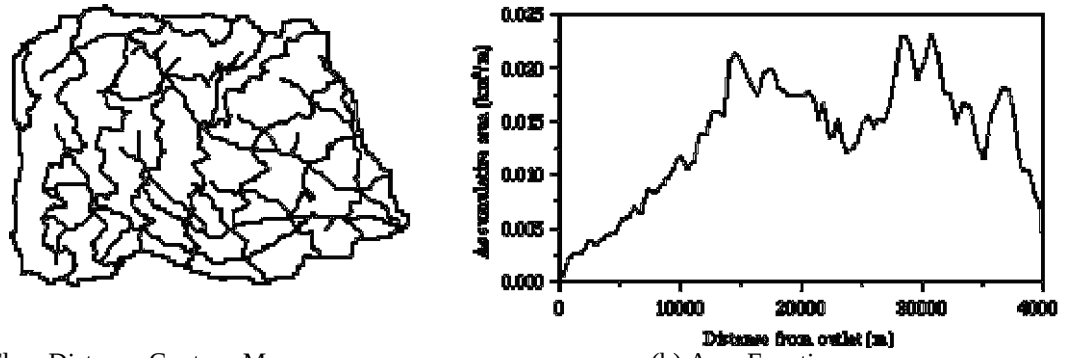

(a) Flow Distance Contour Map (interval is 5 km)

(b) Area Function

Fig. 2 Flow Distance and Area Function of the Example Catchment

Considering the flow interval Δx at distance x, the catchment area accumulated in this interval is given by the area function. In the hydrologic model, the catchment is divided into a number of flow intervals along the flow path. Within each flow interval, there are several river segments. One symmetric hillslope element is assumed to correspond to a river segment. Then a flow interval is represented using a series of hillslope elements. The number of hillslope elements depends on the number of streams within the same flow interval, and the stream number is given by the width function.

3.2 Representation of Spatial Variability

Topography In the hydrological model, the topography is represented using three parameters, i.e. elevation, hillslope gradient and length, which are averaged over each flow interval. The elevation of a flow interval is the average value of all grids within this interval. The hillslope gradient is taken as the average value of the steepest gradients of all grids within the interval. Similar to the area function, these spatial distributions are described by one dimensional distribution functions with respect to the flow distance. Figure 3 shows the elevation and hillslope gradient distribution functions of the example catchment respectively. The hillslope element is assumed as a rectangular inclined plane with width of Δx (same as flow interval length), length of l and angle α. The hillslope length is calculated as

$$l = A(x) / n \qquad (1)$$

where A(x) is the area function at flow distance x (m^2 m^{-1}); n is the number of rivers at flow distance x (given by the width function). The bed rock slope is assumed to be parallel to the surface (Figure 4).

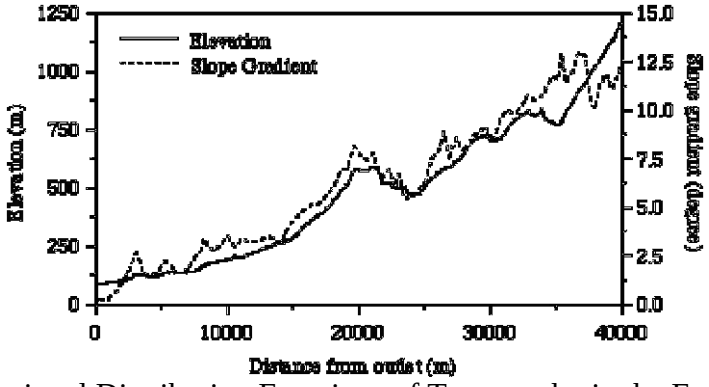

Fig. 3 One-Dimensional Distribution Functions of Topography in the Example Catchment

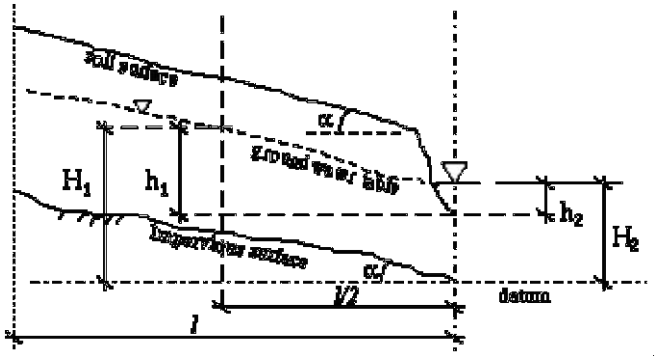

Fig. 4 Hillslope Element in the Hydrologic Model

Land Use and Soil Type Within a flow interval, there may be more than one land use or soil type. Each type of land use or soil takes partial of hillslope element. If a hillslope element contains several types, this element is longitudinally divided into same number of small elements and the unsaturated water flow is simulated independently. The vertical distribution of the soil may not be uniform generally. The non-uniform vertical distribution is represented using an exponential assumption of decreasing of hydraulic conductivity [Jackson et al., 1992], i.e. the hydraulic conductivity decreases with increasing of the soil depth, which is given as

$$K_s(n) = K_0 e^{-fn} \qquad (2)$$

where, $K_s(n)$ is the saturated hydraulic conductivity at depth n (mm h^{-1}), n is the distance taken positive in downward direction normal to surface (m), K_0 is the saturated conductivity at surface (mm h^{-1}), f is parameter (m^{-1}). The soil can be anisotropy specially for forest soil. This anisotropy property is partially led by the distribution of macro pores. The macro pores distribute mainly paralleling to the hillslope. For the anisotropy soil, an anisotropy ratio is defined as [Jackson, et al., 1992].

$$a_r = K_{sp} / K_{sn} \geq 1 \qquad (3)$$

where, a_r is the anisotropy ratio, K_{sp} and K_{sn} is the saturated hydraulic conductivity in the directions normal (n) and parallel (p) to the slope respectively (mm h^{-1}).

Rainfall, Air Temperature and Snow When more than one rain-gauges are available, the rainfall distribution over the catchment is defined by Thiessen polygon. The distribution of each raingauge covering area is described as the same as the area function, designated as rain-area function. Figure 5(a) shows the rain-gauges distributed by Thiessen polygon in Seki River. Figure 5(b) shows the rain-area functions for each rain-gauge. The rainfall value of the flow interval at distance x is given by [Yang, et al., 1997a].

$$r(x) = \sum_{i=1}^{n} r_i A_{r_i}(x) \Big/ \sum_{i=1}^{n} A_{r_i}(x) \qquad (4)$$

where, r_i is the rainfall at *i*th rain-gauge, A_{ri} is the rain-area function of *i*th rain-gauge, n is the number of rain-gauges.

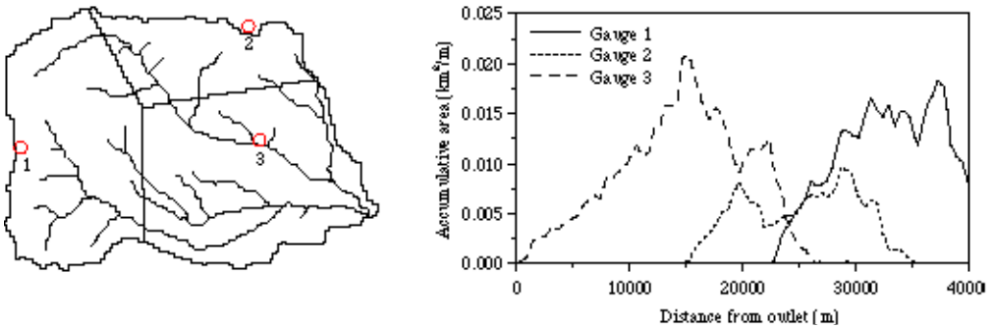

(a) Thiessen Polygon (b) Rain-Area Function

Fig. 5 Rainfall Distribution in the Example Catchment

3.3 Hillslope Hydrologic Model

The hydrologic processes in the hillslope include interception, snowmelt, evapotranspiration, infiltration, overland flow, unsaturated soil water and groundwater flow. In the hillslope hydrologic model, the vertical plane is divided into several layers, including canopy, soil surface, unsaturated zone and groundwater layer (Yang, et al., 1997c).

Canopy Interception For different vegetation or crop species, or on different time periods, the canopy interception ability is different. The Interception capacity S_{c0} at time t is given as

$$S_{C0}(t) = I_0 K_v \frac{L\ A(I)}{L\ A_0 I} \qquad (5)$$

The deficit of canopy water storage is

$$S_{Cd}(t) = S_{C0}(t) - S_c(t) \quad (6)$$

where, S_{C0} is the interception capacity (mm); I_0 is the maximum interception ability of the vegetation in a year (mm); K_v is the vegetation coverage; LAI = the leaf-area-index at time t; LAI_0 is the maximum leaf-area-index of the vegetation in a year; $S_{Cd}(t)$ is the deficit of canopy water storage (mm); $S_c(t)$ is the canopy water storage at time t (mm). Considering the uniform intensity rainfall r(t) in time interval [t,t+Δt], the actual interception is determined as

$$Actual\ interception = \begin{cases} r(t)\Delta t; & r(t)\Delta t \le S_{Cd}(t) \\ S_{Cd}(t); & r(t)\Delta t > S_{Cd}(t) \end{cases} \quad (7)$$

Evapotranspiration Actual evapotranspiration is calculated as evaporation from canopy water storage, transpiration from root zone, evaporation from surface storage and evaporation from soil surface. The evaporation from soil surface is estimated as a function of average soil moisture content in the first layer. The evapotranspiration is assumed take place only during the daytime 12 hours. The daily potential evaporation is divided by 12 hours to convert it to hourly potential evaporation.

Actual evaporation rate from canopy in time interval [t,t+Δt] is given by

$$E_{canopy}(t) = \begin{cases} K_v K_c E_p; & S_c(t) \ge K_v K_c E_p \Delta t \\ S_c(t)/\Delta t; & S_c(t) < K_v K_c E_p \Delta t \end{cases} \quad (8)$$

where, E_{canopy} is the actual evaporation rate from canopy storage (mm h^{-1}); E_p is the potential evaporation rate (mm h^{-1}); Δt is the time interval (h). The vegetation transpiration rate from each soil zone in time interval [t,t+Δt] is written as

$$E_{tr}(t) = \left[K_v K_c E_p\right] f_1(z)\, f_2(\theta) \frac{LAI(t)}{LAI_0} \quad (9)$$

where, $E_{tri}(t,i)$ is the transpiration rate (mm h^{-1}) from zone i at time t; K_c is crop coefficient; f_1 is the root distribution function; $f_2(\theta)$ is soil moisture function; θ is the soil moisture content. The actual evaporation rate from soil water storage in time interval [t,t+Δt] is given by

$$E_{surface}(t) = \begin{cases} E_p(1-K_v); & S_s(t) \ge E_p(1-K_v)\Delta t \\ S_s(t)/\Delta t; & S_s(t) < E_p(1-K_v)\Delta t \end{cases} \quad (10)$$

where, $E_{surface}$ is the evaporation rate from surface water (mm h^{-1}); $S_s(t)$ is the surface water storage at time t (mm). The evaporation rate from soil surface in time interval [t,t+Δt] is given by

$$E_s(t) = \{E_p(1-K_v) - E_{surface}(t)\}\, f_2(\theta) \quad (11)$$

where $E_s(t)$ = the evaporation rate from soil surface (mm h^{-1}).

Unsaturated Zone Water Flow The unsaturated zone water flow is described using one-dimensional Richards equation,

$$\frac{\partial \theta(z,t)}{\partial t} = -\frac{\partial q}{\partial z} + s(z,t) \quad (12)$$

where θ is the volumetric water content, K(θ) is hydraulic conductivity, t is time, s is source or sink; q is the soil moisture fluxes in vertical direction, given as

$$q = -K(\theta, z)\left[\frac{\partial \psi(\theta)}{\partial z} - K(\theta, z)\right] \quad (13)$$

Overland Flow The surface flow along the hillslope elements are simply described by the one dimensional kinematic wave model including the continuity equation

$$\frac{\partial h}{\partial t} + \frac{\partial q_s}{\partial x} = i \quad (14)$$

and momentum equation

$$S_0 = S_f \quad (15)$$

where q_s is the discharge per unit width ($m^3\ s^{-1}\ m^{-1}$); h is water depth (m); t is time (s); x is the distance along the hillslope (m); i is net input (net rainfall and snowmelt) (m); S_0 is the hillslope gradient; S_f is the friction slope gradient. Using Manning type friction slope, the momentum equation is written as

$$q_s = \frac{1}{n} S_0^{1/2} h^{5/3} \quad (16)$$

where n is manning roughness parameter.

Saturated Zone Water Flow and Exchange with River The basic equations used for the saturated zone are mass balance and Darcy's law. The mass balance is give by

$$\frac{\partial S_G(t)}{\partial t} = rech(t) - L(t) - q_G(t)\frac{100}{A} \quad (17)$$

where, $\partial S_G(t)/\partial t$ is the change of groundwater storage (unconfined aquifer) (mm); rech(t) is the recharge rate from upper unsaturated zone ($mm\ h^{-1}$); L(t) is the leakage to deep aquifer ($mm\ h^{-1}$); A is the plane area of hillslope element ($m^2\ m^{-1}$); $q_G(t)$ is the discharge to the river per unit width ($m^3\ h^{-1}\ m^{-1}$), calculated as

$$q_G(t) = K_G \frac{H_1 - H_2}{L/2} \frac{h_1 + h_2}{2} \quad (18)$$

where, K_G is the hydraulic conductivity of unconfined aquifer.

3.4 River Flow

The kinematic wave model given by the continuity and momentum equations is used for river routing and solved using explicit finite difference method.

$$\frac{\partial Q}{\partial x} + \frac{\partial A}{\partial t} = q_L; \qquad q_L = q_S + q_G \quad (19)$$

Momentum equation is given by Manning's equation

$$Q = \frac{S_0^{1/2}}{n p^{2/3}} A^{5/3} \quad (20)$$

where, x is distance along the longitudinal axis of the river (m); t is time (s); A is cross-sectional area (m^2); Q is discharge at x ($m^3\ s^{-1}$); q_L is lateral inflow ($m^3\ s^{-1}\ m^{-1}$); S_0 is the river bed slope; n is Manning's roughness; P is wetting perimeter (m).

3.5 Reservoir Routing

Reservoir routing uses mathematical method to simulate outflow from a reservoir once the inflow, initial conditions, reservoir characteristics (H-V curve), and operational rules are known. There are basically two types of reservoir routing approach, storage-based routing and hydraulic routing. For hydrologic purpose, reservoir routing commonly uses the storage concept. By the mass conservation principle, the change of storage per unit time is balanced by the inflow and outflow, in the differential form as

$$\frac{dS}{dt} = I - O \tag{21}$$

where I is inflow, O is outflow, and S is the storage.

The finite difference form is written by the simplest way as following

$$\frac{I_1 + I_2}{2} - \frac{O_1 + O_2}{2} = \frac{S_2 - S_1}{\Delta t} \tag{22}$$

where the lower index '1' indicates the current time level and '2' indicates the next time level; Δt is time interval. Replacing the term $(O_1 + O_2)/2$ in equation 22 by the mean outflow $\bar{O}$, we obtain

$$\bar{O} = \frac{S_2 - S_1}{\Delta t} + \frac{I_1 + I_2}{2} \tag{23}$$

where S_1 is the actual storage at current time level; S_2 is the operational storage at next time level according the reservoir operation curve; I_1 is the inflow at current time level; I_2 is the inflow at next time level; Δt from time level 1 to 2. The outflow should be not less than the minimum release which is required to maintain the river nature functions. The reservoir operation can be carried daily, weekly or monthly.

3.6 Treatment of Large Catchments

Since the topographical parameters and other spatial variations used in the hydrologic model are averaged over the flow intervals, this aggregating procedure may introduce large error into the hydrologic simulation in large catchments. For large catchment, it should be divided into a number of sub-catchments. The size of the sub-catchment may depend on the topography or the simulation requirements.

The river network of each sub-catchment is lumped as a single "equivalent" channel (represented using the main river). A simplified river network is obtained in the whole catchment and used in river routing simulation to obtain whole catchment response. other hydrologic processes are simulated independently in each sub-catchment.

4. Comparison of Grid and Geomorphology Based Distributed Hydrologic Models

4.1 Study Area

In order to compare the representation of spatial variations and investigating the performance of both models, we select Seki River as the study area which is located in Hokuriku region of Japan and has an area of 703 km^2. One land use type (forest), one soil type (Kanto loam) and uniform depth of unconfined aquifer are considered within this catchment. In this case, the topography is the only spatial varying information. The DEM resolution which is used by the two hydrological

models is 300 m resampled from original 250 m cell size data (Yang et al., 1998b).

4.2 Representation of Spatial Variations in the Two Models

The grid size used in MIKE SHE is 300 m, the geomorphology-based model (designated GB model) uses 119 flow intervals which have the length of 300-600 m. Table 1 shows the representations of the catchment by the two models. The discrete units are uniform in MIKE SHE, but vary with flow distance in GB model. The total number of grids used in MIKE SHE is 7830 and the total hillslope element number in GB model is 1018. On the elevation and slope gradient of the discrete unit, the minimum values are same in both models; the mean values are very close; but maximum value in MIKE SHE is greater than GB model. The maximum slope gradient in MIKE SHE is 63.4%, but 28.8% in GB model.

Table 1 Representation of Catchment

Model	Discrete unit			Elevation (m)			Slope gradient (%)		
	number	length (m)	area (km^2)	min.	max.	mean	min.	max.	mean
MIKE SHE	7830	300X300 (uniform)	0.09	9.99	2329.4	712.6	0.0	63.4	14.7
GB model	1018	825.4X480.7 (mean)	0.789	10.0	2228.0	730.7	0.0	28.8	13.7

4.3 Comparison of Model Performance

The two models were applied in Seki River with same conditions. The rainfall, air temperature and sunshine hours are from AMeDAS data source. There are four rain-gauges, two of them had the air temperature and sunshine hour records. MIKE SHE runs from November 1, 1994 to December 31, 1995; GB model runs from January 1, 1994 to December 31, 1995. Because of the uniform land use and soil, GB model treats the vertical direction within a flow interval by a single soil column; the number of soil columns is same as flow interval number. MIKE SHE also regroup the soil columns according to the meteorological input, vegetation type and soil type; and the maximum number of unsaturated columns that can be simulated in MIKE SHE is 300. Both simulations output hourly results. Figure 6 shows the comparison of daily hydrographs of 1995 simulated by MIKE SHE and GB model with the observed one. The daily discharge errors from MIKE SHE simulation are manly from April to June, the simulated discharge is smaller than observed one. The snow and air temperature are distributed by Thiessen polygon as same as rainfall in MIKE SHE, this may introduce the above error. The errors from GB model simulation are mainly from end of July to August, the simulated hydrograph is lower than the observed one. Probably, this error is brought by the simpler groundwater description. Table 2 summaries the simulation results of 1995 by both models. The total actual evapotranspiration, total river outflow and the daily discharge error by the two models are very close. We can see that the simulation results by GB model is as good as MIKE SHE, but the computation time of GB model is only 0.3% of that MIKE SHE spent.

The results shows that GB model is good as the comprehensive distributed MIKE SHE, and it takes much less computation time than MIKE SHE. Due to the fast computation advantage, the geomorphology-based hydrologic model can be apply to large scale.

Table 2 Comparison of Model Performance

Model	Actual	Total River	Error (%)	Computation

Type	Evapotranspiration (mm)	Outflow (mm)	total outflow	daily discharge	Time (hr) (work station)
MIKE SHE	787.0	2164.5	-10.0	17.6	72
GB model	780.8	2050.8	-14.8	17.5	1/6

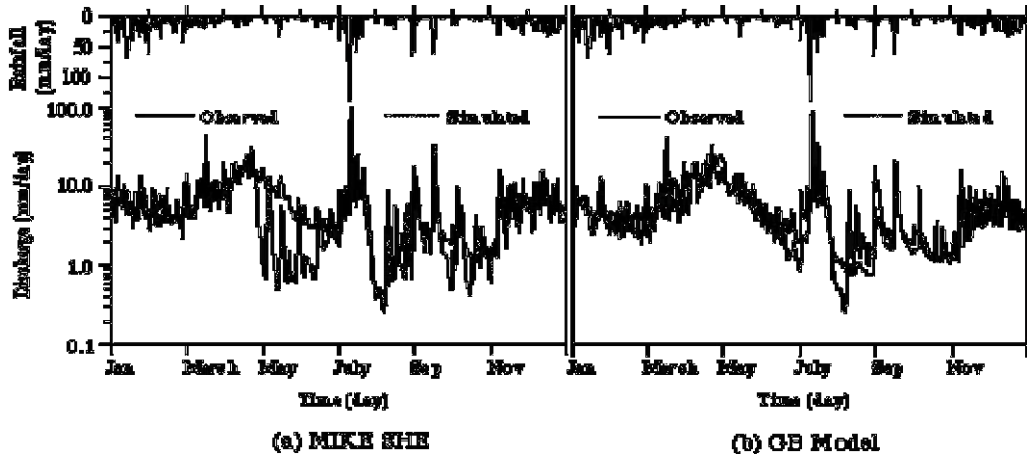

Fig. 6 Comparison of Daily Hydrographs of 1995 Between Simulated and Observed

5. Application of Geomorphology-Based Model to Chao Phraya River Basin

5.1 Description of Chao Phraya River Basin in Thailand

Chao Phraya river is the largest river (both the basin area and river length) in Thailand. It originates from north high mountain, drains through the central plan and finally discharges to the Gulf of Thailand. The whole river basin has an area near 200,000 km^2 and covers one-third of whole country area. The upper four main sub-catchments namely Ping river, Wang river, Yom river and Nan river join at Nakhon Sawan and the cumulative area is 110,569 km^2 (the simulation area in the study). Two main reservoirs are located on Ping river and Nan river, namely Bhumibol and Sirikit reservoir. Figure 7 shows the location of Chao Phraya river basin in Thailand.

The climate is tropic monsoon, marked by a pronounced rainy season lasting from about May to September and relatively dry season for the remainder of the year. The mean annual precipitation is about 1,200 mm. The monsoon season rainfall is around 90% of the annual rainfall.

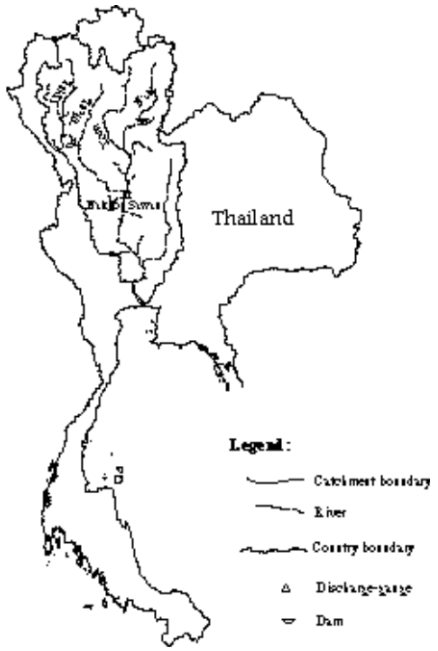

Fig. 7 Location of Chao Phraya River Basin in Thailand}

5.2 Input Data

Meteorological Data The meteorological data available in this catchment include rainfall and pan evaporation which are collected from Royal Irrigation Department of Thailand. There are 140 rain gauges which have only daily rainfall records and 11 pan evaporation gauges in the study area. Two-years (1994-1995) data set is selected for the application, which has relatively few missing data. The missing data in the data set is filled using the nearest records at same time. Hourly rainfall data are needed for hydrologic simulation and estimated by dividing by the rain duration. The rain duration is assumed to be equal at night and daytime and related to daily rain amount. The duration is assumed to be 6 hours for the daily rainfall less than 10 mm; 12 hours for daily rainfall ranges 10-30 mm; 24 hours for daily rainfall more than 30 mm. The distributions of rain gauge and evaporation pan are not uniform, few gauges locate in mountainous area. Figure 8 shows the distributions of rain gauges and evaporation pans in the study area.

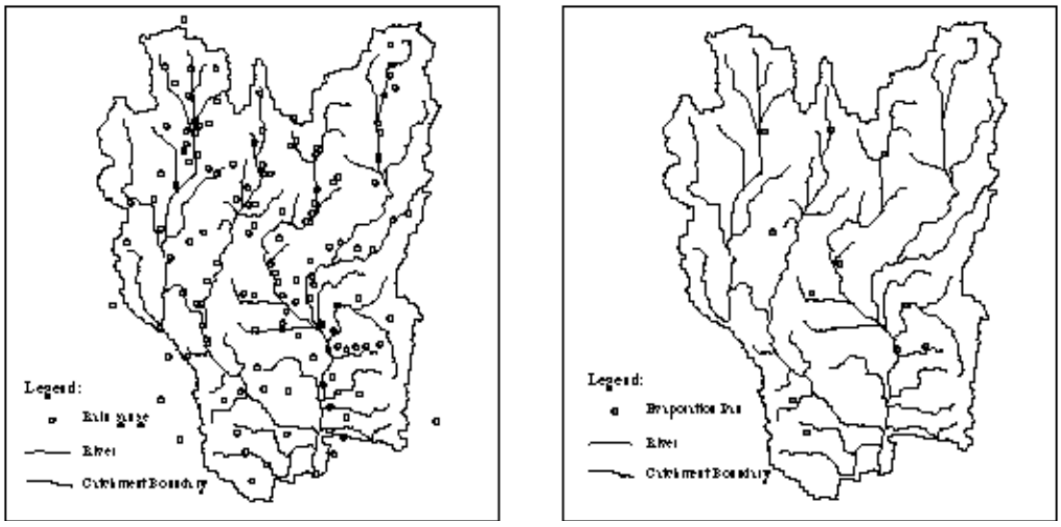

(a) Distribution of Rain Gauges (b) Distribution of Evaporation Pans

Fig. 8 Meteorological Data Available in the Study Area

Topographical and Geological Data The topographical and geomorphologic parameters are extracted from DEM, available digital elevation data in this region is 30 second (approximately 1 km) resolution which is from EROS (the Earth Resources Observation Systems) Data Center Distributed Active Archive Center (EDC DAAC) of U.S. Geological Survey (web site: http://edcwww.cr.usgs. gov/landdaac/). Due to the coarse resolution, the DEM can not precisely represent the actual topography. This introduces error to the topographical and geomorphological parameters. No geological data is available, so the top soil depth is assumed to be uniform and of 2 m, and no aquitard is specified. The field surveyed data of seventeen cross-sections of the main rivers are available. The shape of most cross-sections are close to rectangle, so all rivers are assumed to be rectangular.

Land Use and Soil Water Parameters The digital versions of land use and soil maps were prepared by the GAME project (from Global Engineering Laboratory, Institute of Industrial Science, University of Tokyo). The land use map was classified from LANDSAT TM images of 1990 and produced as 11 categories map of 5 second resolution. The soil map was digitized from the 1:1,000,000 soil map offered by Land Development of Thailand, which has same resolution as land use map and very detail categories (44 soil types in the study area). Soil water properties were measured from the soil samples in laboratory and mainly from two sources, one is Department of Soil Science, Kasetsart University, Thailand; another one is GAME project (from Hydrology and Water Resources Laboratory, Institute of Industrial Science, University of Tokyo). These soil samples were collected from different types of land use, so the soil parameters were given for soil of different land uses. It is different to directly use the soil map even it has very detail soil types. By comparing the soil map with land use map, there are some relations between the two maps. Within one land use type, there is one main soil type covers most of the area or those soils can be classified into one group. In this study, the land use map is used instead of soil map, and reclassified into 5 categories by merging some very similar types and very small types. The reclassified land use map is shown in Figure 9. The soil water parameters used in the study are given in Table 3. Other parameters corresponding to each land use type are given in Table 4. Leaf-Area-Index for each crop or vegetation is given in Table 5.

Fig. 9 Land Use Map of the Study Area in Chao Phraya River Basin

Table 3 Soil Water Parameters of the Study Area in Chao Phraya River

Soil Type	θ_s	θ_r	θ_f	θ_w	α	n	K_{s0}	K_{s1}	K_{s2}	a_r
Irrigated Paddy	0.3801	0.021	0.3	0.021	0.0618	1.1772	3	1	1	1
Non-irrigated Paddy	0.3801	0.021	0.3	0.021	0.0618	1.1772	3	1	1	1
Upland Field	0.3705	0.084	0.3	0.084	0.2339	1.1223	3	1	1	1
Orchard Field	0.3869	0.033	0.29	0.033	0.0749	1.5046	10	3	2	2
Forest Land	0.3831	0.016	0.29	0.016	0.185	1.1742	30	5	5	5

Notes:

θ_s --- saturated soil moisture content; θ_r --- residual soil moisture content;
θ_f --- soil moisture content at field capacity; θ_w --- soil moisture content at wilting point;
α, n --- parameters in Van Genuchten's Equation , another parameter m=1-1/n;
K_{s0} --- saturated hydraulic conductivity of the first layer of top soil zone;
$K_{\_s1}$ --- saturated hydraulic conductivity of bottom layer of top soil zone;
$K_{\_s2}$ --- hydraulic conductivity of groundwater;
a_r --- anitropic ration in Equation (3)
Storage coefficient of groundwater is 0.1.

Table 4. Parameters of Different Land Uses in Study Area of Chao Phraya River

Month	Surface Stora ge (mm)				
	Irrigated Paddy	Non-irrigated Paddy	Upland	Orchard	Forest
Jan.	30	30	30	30	20
Feb.	30	30	30	30	20
Mar.	30	30	30	30	20
Apr.	50	30	30	30	20
May	80	30	30	30	20
June	100	50	30	30	20
July	100	100	30	30	20
Aug.	100	100	30	30	20
Sep.	100	100	30	30	20
Oct.	100	100	30	30	20
Nov.	100	50	30	30	20
Dec.	50	30	30	30	20
Vegetation Coverage (%)					
	80	80	90	70	60
Maximum Canopy Storage (mm)					
	1	1	1	2	2
Kpan					
	0.85	0.85	0.8	0.75	0.75

Table 5. Leaf-Area-Index for Different Vegetation in Chao Phraya

Month	Leaf-Area-Index LAI/LAI0				
	Rice (irrigated)	Rice (non-irrigated)	Upland Crop	Orchard Tree	Forest
Jan.	0.2	0	0.2	0.6	0.6
Feb.	0.1	0	0.2	0.6	0.6
Mar.	0.2	0	0.2	0.8	0.8
Apr.	0.3	0.2	0.2	1	1
May	0.6	0.4	0.2	1	1
June	1	0.6	0.8	1	1
July	0.5	0.8	0.8	1	1
Aug.	0.6	0.8	0.8	1	1
Sep.	1	1	0.8	1	1

Oct.	1	1	0.8	0.8	0.8
Nov.	0.6	0.8	0.8	0.6	0.6
Dec.	0.3	0.2	0.2	0.6	0.6

5.3 Reservoir, Irrigation Weir and River Discharge Gauges

There are dams, irrigation weirs and regulation gates on the main rivers within the study area of Chao Phraya river basin. But data are available only for two main reservoirs and two main irrigation weirs. The two main reservoirs are Bhumibol reservoir on Ping river and Sirikit reservoir on Nan river, and the two main irrigation weirs are Khamphang Khet Weir and Phitsanulok Weir (Figure 10a). Daily river discharge data are available at 24 gauges (Figure 10b), these data are for comparison with the model simulations.

Bhumibol reservoir has a catchment area of 26,386 km^2 and gross storage capacity of 13,462 MCM. Sirikit reservoir has a catchment area of 13,130 km^2 and gross storage capacity of 10,500 MCM. Figure 11 (a) and (b) show the water level and capacity curves of the two reservoirs. The main purposes of the both reservoirs are for power generation, irrigation and flood control. The monthly water level variation curve of the simulation period (1994-1995) is used as the operational curve (Figure 12 a and b). The daily intake discharge data from both irrigation weirs are available in some years. Monthly average intake discharge is taken as the boundary condition in river network routing. Figure 13 shows the intake discharge from the two weirs. Corresponding to both irrigation weirs, there are two main irrigation areas within the study area. The irrigated water is distributed uniformly and treated as rainfall in the simulation.

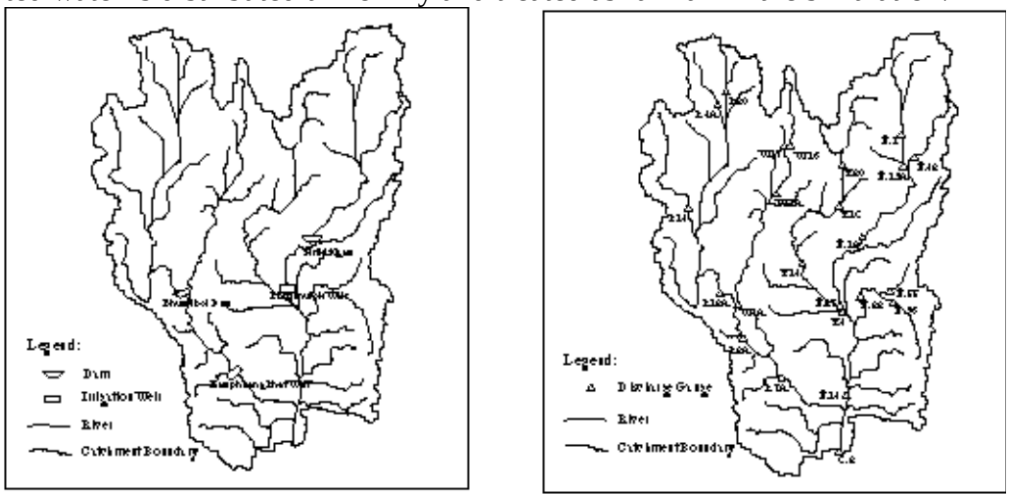

(a) Reservoirs and Irrigation Weirs (b) Discharge Gauges

Fig. 10 River Data Used in Hydrologic Simulation

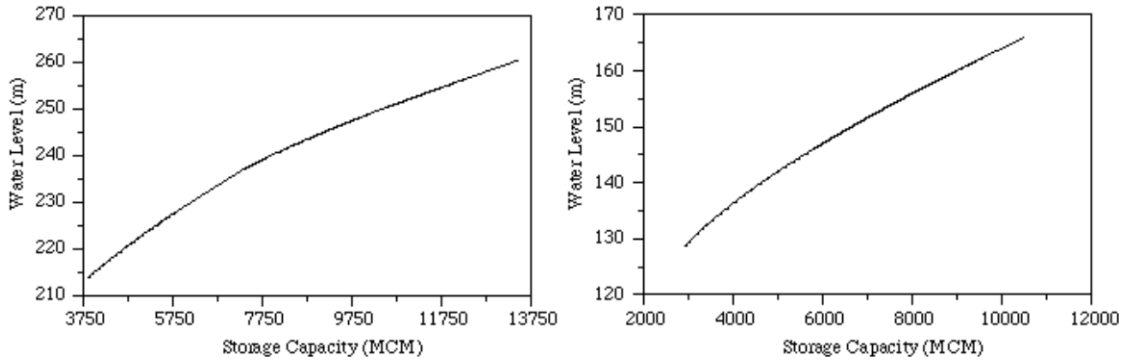

(a) Bhumibol Reservoir (b) Sirikit Reservoir

Fig. 11Water Level-Storage capacity Curve of Reservoir in Chao Phraya river

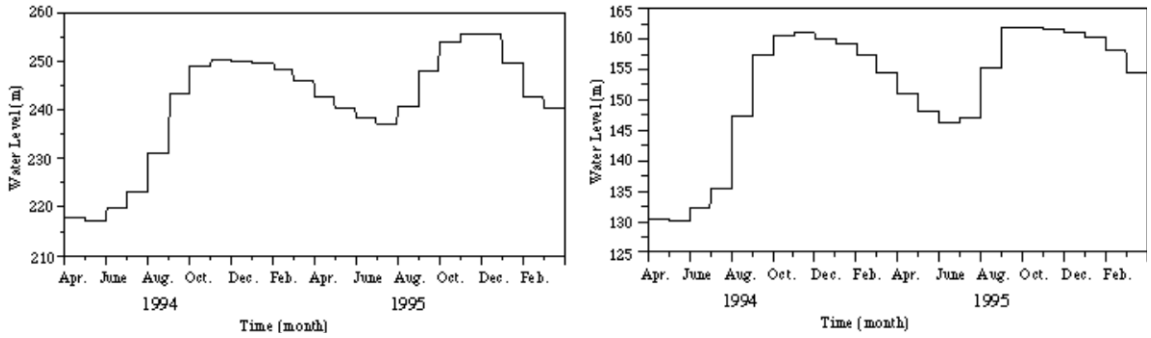

(a) Bhumibol Reservoir (b) Sirikit Reservoir

Fig. 12 Operation Curve of Reservoir in Chao Phraya river

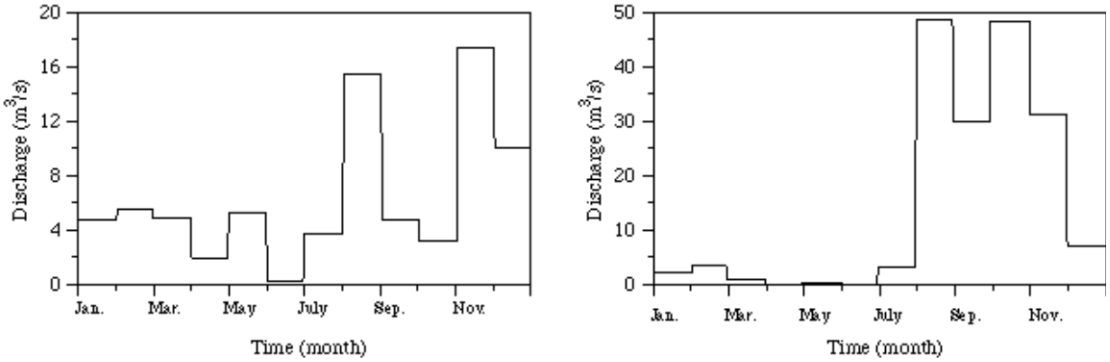

(a) Khamphang Khe Weir (b) Phitsanulok Weir

Fig. 13 Monthly Intake Discharge from Irrigation Weir in Chao Phraya river

5.4 Results and Discussion

Hourly simulations are carried out from hydrologic year (April to next March) 1994 to 1995. Simulation results include river discharge at each gauge, reservoir release and spatial distributions of hydrologic characteristics.

River Discharge and Reservoir Release The model output daily discharge at 24 gauges (see Figure 10b). Figure 14 shows the Bhumibol reservoir inflow, release and water level. Figure 15 shows the comparisons of daily hydrographs between simulated and observed at two gauges near Nakhon Sawan. The simulated results of reservoir releases agree the general pattern of the actual releases, the simulated release processes are smoother than the actual ones because weekly operation is adapted in reservoir routing which is based on monthly average operational curve. The simulated reservoir water level agrees the actual level very well. It can be seen that the reservoir operation during flood period can not be simply described by the monthly operational curve, the extra operation rule is necessary for reservoir flood routing. Generally, the agreements of the hydrographs between simulated and observed during the rain season are better than that during the dry season, and the simulated discharge before the rain season is lower than actual value at the upper stream (Ping, Wang, Yom and Nan sub-catchments). At the lower part, the main differences of hydrographs between the simulated and observed are mainly in the peak, the simulated peak responses are earlier and lower than the actual ones. This may be caused by the flat topography and large amount of surface storage.

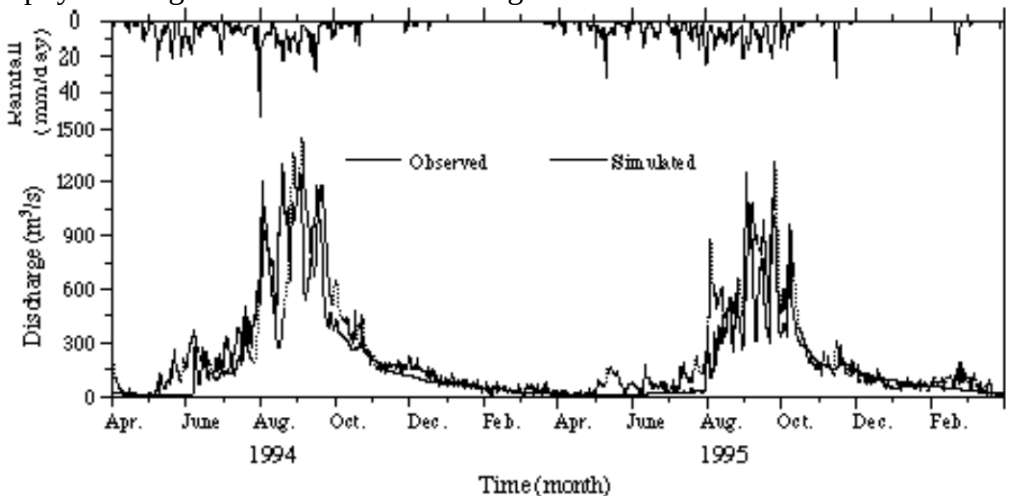

(a) Gauge P12.A (Bhumibol Reservoir Inflow)

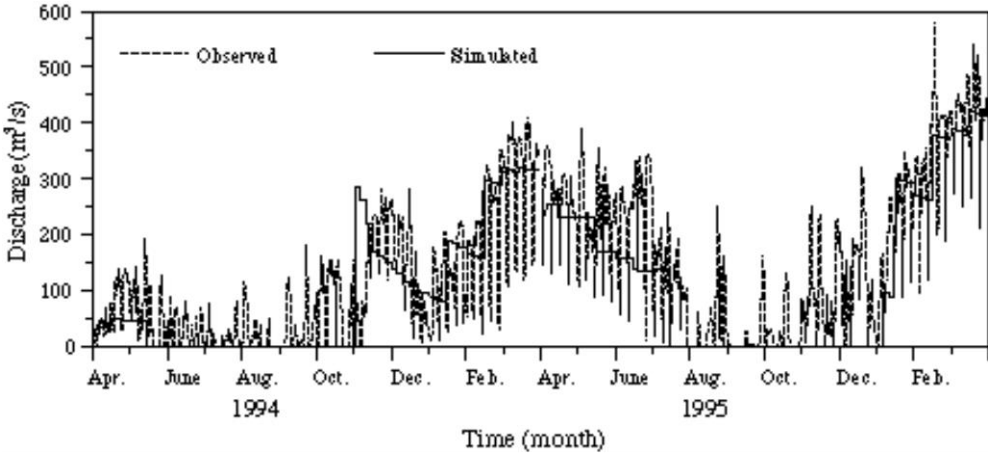

(b) Gauge P12.A (Bhumibol Reservoir Release)

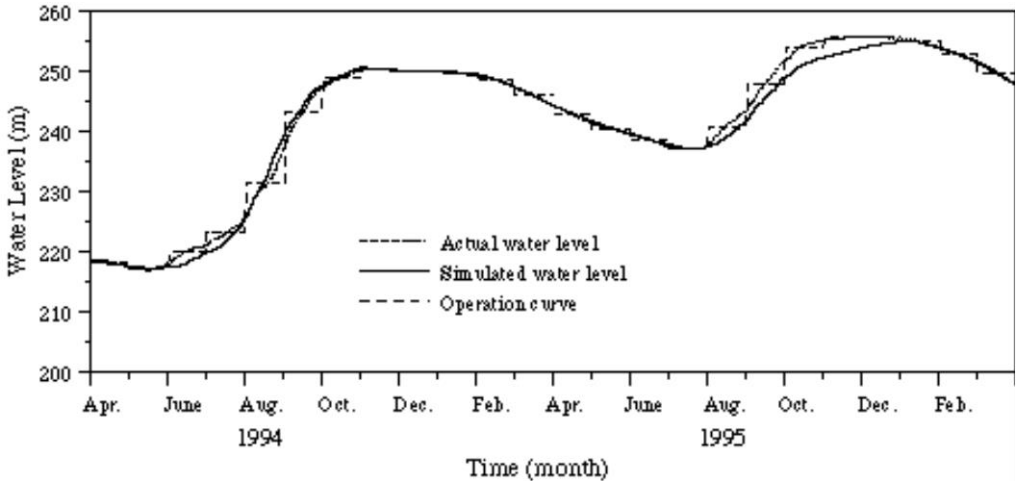

(c) Water Level of Bhumibol Reservoir

Fig. 14 Simulation Results of Bhumibol Reservoir

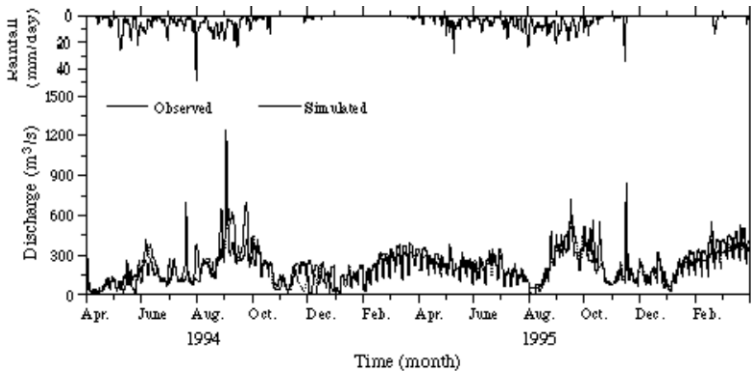

(a) Gauge P.7A

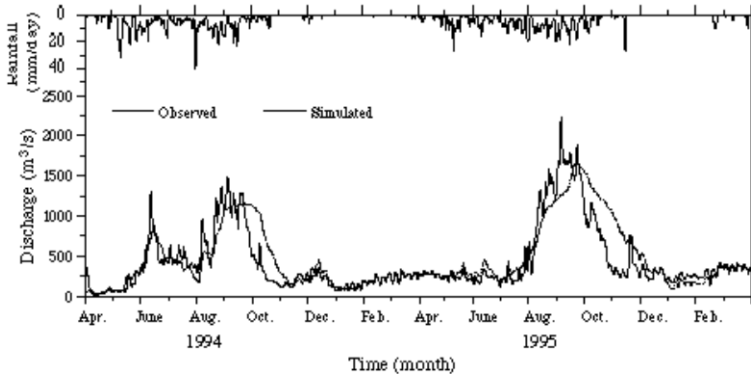

(b) Gauge N.14

Fig. 15 Daily Hydrographs at Two Gauges Near Nakhon Sawan}

Spatial Distributions of Hydrologic Characteristics The distributions of monthly total evapotranspiration and average soil moisture content are compared. Figure 16 shows the

distributions of actual evaporation of each month in hydrologic year 1994. The actual evapotranspiration is relatively higher during May to October. The depth of unsaturated soil layer used in the simulation is 0.5 m. The soil moisture content is given by average value for each layer. The variations of soil moisture of the top layer are important for crops and evaporation. Corresponding to Figure 16, the distributions of top layer soil moisture of each month in 1994 are shown in Figure 17. The top soil is relatively wet during May to October.

Fig. 16 Distributions of Monthly Total Actual Evapotranspiration (in mm) of Chao Phraya River Basin in Hydrologic Year 1994

Fig. 17 Distributions of Monthly Average Soil Moisture Contents (θ/θ_s, in %) of Top 50 cm Zone in Chao Phraya River Basin in Hydrologic Year 1994

Water Management with Reservoir The main water use in Chao Phraya river basin is irrigation. The reservoir operation is designed maily according to the irrigation demands. Considering the paddy field in Ping river and Wang river up to Gauge P.7A, the monthly changes of water demands (=irrigation demand + evaporation - rainfall), river flow without reservoir regulation and river flow with reservoir (Bhumibol reservoir) regulation are shown in Fig. 16. It clearly shows that river water can not satisfy the irrigation demands during the dry season if there is no reservoir. Bhumibol reservoir stored the water during the rain season and released water for irrigation during the dry season.

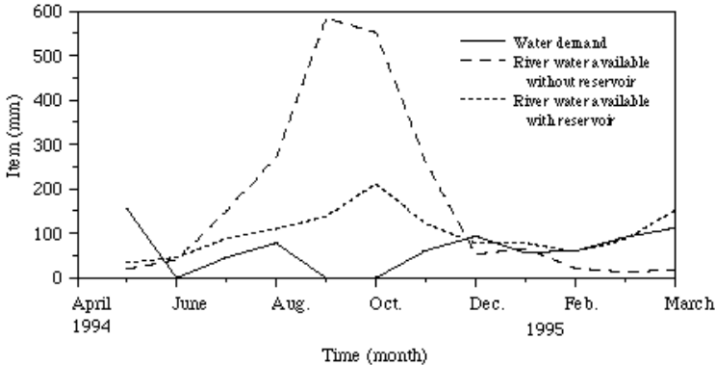

Fig. 16 Water Management with Reservoir

6. Conclusions

In the present developed hydrologic model, a discrete flow interval-hillslope system is used and the computational unit is hillslope element instead of the grid element used in the grid-based distributed model. The hydrologic model is based on the one dimensional representations of catchment spatial variations by using the catchment geomorphological area function concept. The lateral dimension of the catchment is reduced from two to one dimension and the river network is lumped as a single equivalent channel.

The model was applied to Chao Phraya river basin in Thailand which is located in tropical monsoon region. The simulation area is about 110,000 km^2 (up to Nakhon Sawan). The hydrologic simulation has been carried out during 1994-1995 including two large reservoirs. The model outputs include both river discharge and spatial distributions of hydrologic characteristics. The computation time spent by the present model is only 1/50 of that taken by previous grid-based hydrologic model for same simulation. Due to the faster computation advantage, this

model can be applied to regional scale and also used for reservoir optimal operation.

References

Beven, K. A. Claver, and E. Morris eds., *The Institute of Hydrology Distributed Hydrological Model*, Institute of Hydrology, Report 98, Willingford, UK, 1987

Beven, K., Changing Ideas in Hydrology -- The Case of Physically-Based Models, *Jounal of Hydrology*, 105, 157-172, 1989

Jackson, C., Hillslope Infiltration and Lateral Downslope Unsaturated Flow, *Water Resources Research*, 28(9), 2533-2539, 1992

Naden, P., Spatial Variability in Flood Estimation for Large Catchments: the Exploitation of Channel Network Structure, *Hydrological Science Journal*, 37, 53-71, 1992

Refsgaard, J. and Storm, MIKE SHE, in Sing, V. ed., *Computer Models in Watershed Hydrology*, Water Resources Publication, 1995

Yang, D., S. Herath, and K. Musiake, Analysis of geomorphologic properties extracted from DEMs for hydrologic modeling, *Annual Jounal of Hydraulic Engineering, JSCE*, Vol. 41, 105-110, 1997a

Yang, D., S. Herath, and K. Musiake, Simulation of Catchment Rainfall-Runoff Using Area Function and Tank Model, in *Proceeding of 1997 Annual Conference, JSCE*, Vol. 2, 324-325, 1997b

Yang, D., S. Herath, K. Musiake, and T. Nakaegawa, Development of a simplified physicall-based hillslope model for modeling flood in mountainous catchments, in *Proceeding of 1997 Annual Conference, Japan Society of Hydrology and Water Resources*, 57-58, 1997c

Yang, D., S. Herath, and K. Musiake, Development of A Geomorphology-Based Hydrological Model for Large Catchments, *Annual Jounal of Hydraulic Engineering, JSCE*, Vol. 42, 169-174, 1998a

Yang, D., S. Herath, and K. Musiake, Comparison of grid and geomorphology based distributed hydrological models, in *Proceeding of 1998 Annual Conference, JSCE*, Vol. 2, 72-73, 1998b